Research Square

Preprints are preliminary reports that have not undergone peer review.
They should not be considered conclusive, used to inform clinical practice,
or referenced by the media as validated information.

IL-22 hinders antiviral T cell responses and exacerbates neurological disorders in ZIKV-infected immunocompetent neonatal mice

Yuejin Liang (yu2liang@utmb.edu)
University of Texas Medical Branch at Galveston https://orcid.org/0000-0002-9557-1847
Panpan Yi
Xiangya Hospital Central South University
Wenjuan Ru
University of Texas Medical Branch at Galveston
Zuliang Jie
MD Anderson Cancer Center
Hui Wang
University of Texas Medical Branch at Galveston
Tamer Ghanayem
University of Texas Medical Branch at Galveston
Xiaofang Wang
University of Texas Medical Branch at Galveston
Edrous Alamer
University of Texas Medical Branch at Galveston
Jinjun Liu
University of Texas Medical Branch at Galveston
Haitao Hu
University of Texas Medical Branch at Galveston
Lynn Soong
University of Texas Medical Branch at Galveston
Jiyang Cai
University of Oklahoma health science center
Jiaren Sun
University of Texas Medical Branch at Galveston

Research

Keywords: ZIKV, IL-22, Astrocytes, Brain, Microglia, Encephalitis, Neonatal mice, CD8

Posted Date: June 2nd, 2020

DOI: https://doi.org/10.21203/rs.3.rs-31941/v1

License: This work is licensed under a Creative Commons Attribution 4.0 International License.
Read Full License

Version of Record: A version of this preprint was published on August 25th, 2020. See the published version at https://doi.org/10.1186/s12974-020-01928-9.

Abstract

Background

The Zika virus (ZIKV) outbreak that occurred in multiple countries was linked to increased risk of neurological disorders and congenital defects. However, host immunity and immune-mediated pathogenesis in ZIKV infection are not well understood. Interleukin-22 (IL-22) is a crucial cytokine for regulating host immunity in infectious diseases. Whether IL-22 plays a role in ZIKV infection is unknown.

Methods

The cellular source of IL-22 was identified in IFNAR$^{-/-}$ mice and WT neonatal mice during ZIKV infection. To determine the role of IL-22, we challenged 1-day-old wild-type (WT) and IL-22$^{-/-}$ mice with ZIKV and monitored clinical manifestations. Glial cell activation in the brain was assessed by confocal imaging. ZIKV-specific CD8^{+} T cell responses in both the spleen and brain were analyzed by flow cytometry. In addition, we infected mouse primary astrocytes *in vitro*, and characterized the reactive astrocyte phenotype. Human glial cell line was also infected with ZIKV in the presence of IL-22, followed by the evaluation of cell proliferation, cytokine expression and viral loads.

Results

We found that γδ T cells were the main source of IL-22 during ZIKV infection in both the spleen and brain. WT mice began to develop weight loss, staggered steps, bilateral hind limb paralysis, weakness at 10 days post-infection (dpi), and ultimately succumbed to infection at 16–19 dpi. Surprisingly, IL-22 deficiency lessened weight loss, moderated the systemic inflammatory response, and greatly reduced the incidence of neurological disorders and mortality. ZIKV infection facilitated a neurotoxic polarization of A1-prone astrocytes *in vitro*. Additional analysis demonstrated that the absence of IL-22 resulted in reduced activation of microglia and astrocytes in the cortex. Although IL-22 displayed a marginal effect on glial cells *in vitro*, IL-22$^{-/-}$ mice mounted more vigorous ZIKV-specific CD8^{+} T cell responses, which led to a more effective control of ZIKV in the brain.

Conclusions

Our data revealed a pathogenic role of IL-22 in ZIKV encephalitis.

Background

Zika virus (ZIKV) is an emerging mosquito-transmitted flavivirus that has caused severe disease in developing fetuses and immunocompromised adults [1–3]. ZIKV infection is a major concern for public

health by virtue of its spread to South and Central America in 2014, leading to thousands of human infections in Brazil [4]. Although most adults infected with ZIKV experience a mild influenza-like illness, including fever, headache, rash, conjunctivitis and joint pain, a minority develop severe neurological disorders, such as Guillain-Barré syndrome and fatal encephalitis [5]. ZIKV infection also can transmit from the placenta to the fetus in pregnant women and cause gestational abnormalities, including spontaneous abortion, stillbirth, hydrocephaly and microcephaly [2, 6]. Recent studies demonstrate that several types of brain cells are the targets of ZIKV infection. ZIKV can infect human neural progenitor cells and prevent normal brain growth [7, 8]. Microglia are highly susceptible to ZIKV infection, and they increase inflammatory cytokine production in response [9], indicating the important role of microglia in the pathogenesis of congenital ZIKV infection. Astrocytes are critical for host defense during ZIKV infection, as they are the first cells targeted by ZIKV in the brain of immunocompetent mice [10]. However, ZIKV-infected astrocytes display limited immune responses and may contribute to neuronal infection during later stages by releasing virus [10, 11]. However, key molecules that mediate ZIKV encephalitis are poorly understood.

IL-22 belongs to IL-10 family and is mainly produced by Th17 cells, Th22, γδ T cells, NKT cells, and innate lymphoid cells. IL-22 primarily targets non-hematopoietic cells, including epithelial, stromal cells and hepatocytes, and promotes cell proliferation and tissue regeneration [12]. IL-22 is reported to play a key role in several inflammatory diseases, such as drug-induced acute hepatitis, inflammatory bowel diseases, pneumonia, asthma, and renal ischemia-reperfusion injury [13]. Accumulating evidence show that IL-22 contributes to viral infection. We have demonstrated that IL-22 induced atrophy in lymphoid organs, which resulted in poor antiviral T cell responses in lymphocytic choriomeningitis virus (LCMV) infection [14]. In a lethal West Nile virus (WNV) encephalitis mouse model, IL-22 deficiency resulted in reduced viral load, decreased inflammatory infiltration and alleviated tissue pathology [15]. In addition, IL-22 was increased in multiple sclerosis patients [16] and could disrupt blood-brain barrier (BBB) tight junctions [17]. These studies suggest that IL-22 may play a detrimental role in the central nervous system (CNS) during viral infection. However, whether IL-22 contributes to ZIKV-induced encephalitis and the underlying mechanisms are not entirely known.

In this study, we found that γδ T cells were the main source of IL-22 in the brain and spleen. We found increased animal survival, alleviated clinical symptoms and reduced viral burden in the neonatal IL-22$^{-/-}$ mice compared with those in WT mice. Interestingly, ZIKV infection induced microglia activation and promoted the polarization of A1-prone astrocytes, which were considered neurotoxic [18]. Although IL-22 exhibited a dispensable role for glial cell activation and infection *in vitro*, the lack of IL-22 resulted in decreased microglia activation *in vivo*. Importantly, IL-22$^{-/-}$ mice mounted more effective ZIKV- specific T cell responses *in vivo*, while recombinant IL-22 treatment hindered these responses. Together, our study indicates that IL-22 signaling may play a detrimental role in encephalitis in the ZIKV-infected neonatal mice.

Methods

Mouse experiments

C57BL/6 (JAX stock #000664) and IFNAR$^{-/-}$ (MMRRC stock #32045) mice were purchased from Jackson Laboratory. IL-22$^{-/-}$ mice were kindly provided by Genentech Inc. Mice were housed under 12-hour day/night cycle in the specific pathogen-free, AAALAC-accredited animal facility of UTMB.

ZIKV (Asian lineage FSS13025) was obtained from the World Reference Center for Emerging Viruses and Arboviruses (Galveston, TX). Virus was amplified in Vero cells and viral titer was calculated as fluorescent focus units (FFU) per ml. All newborn mice were born from pathogen-free parents and inoculated one day after birth with 4×10^3 FFU ZIKV in 2 µL by Hamilton microliter syringes through subcutaneous (*s.c.*) inoculation at the lateral side of body part. For *in vivo* treatment, neonatal WT mice were *s.c.* injected with recombinant IL-22 treatment (1 µg in 5 µL, *s.c.*) every other day. In some experiments, mice that were 3 weeks old were intraperitoneally infected with 1×10^5 FFU ZIKV. Animals were monitored daily for bodyweight changes and clinical signs of pathology. Moribund animals were euthanized in accordance with the UTMB IACUC guidelines.

Clinical Symptom Evaluation

The clinical evaluation of infected neonatal mice was modified according to another report [19]. Briefly, Mice were weighed and examined for signs of infection daily. Examination criteria included appearance, stance, and motility. The description of clinical presentations included stagger step (increased spread of hind legs and unusual pauses during movement), paralysis (loss of muscle function of one or two hind legs), and seizure (sudden stiffening of muscles in the back and legs).

Cell Lines And Primary Mouse Glial Cells

Vero and U-87 MG cells were cultured in Minimum Essential Medium (Thermo Fisher Scientific) supplemented with 10% fetal bovine serum. All cells were cultured in the presence of 100 U/mL penicillin and 100 µg/mL streptomycin in 37 °C incubator with 5% CO_2 and 95% humidity control.

For primary mouse glial cell preparation, B6 mouse pups (1–4 days old) were used for mixed cortical cell isolation [20]. Briefly, mouse brains were taken out and placed into a dish containing cold HBSS. The meninges from the cortex hemispheres were pulled with the fine forceps under a stereomicroscope to avoid contamination with meningeal cells and fibroblasts. The cortex hemispheres were cut into small pieces, followed by 2.5% trypsin digestion for 30 min at 37 °C. Cortex tissue pieces were harvested and dissociated into a single-cell suspension. Mixed cortical cells were counted and cultured with DMEM/F12 (1:1) medium plus 10% fetal bovine serum, 100 U/mL penicillin and 100 µg/mL streptomycin in a T75 culture flask. Medium was replaced every 5 days. For microglia isolation, the mild trypsinization method was used. Briefly, mixed cortical cells were cultured for 12–15 days and incubated with a trypsin solution (0.25% trypsin, 1 mM EDTA in HBSS) diluted 1:4 in DMEM/F12 medium. The upper layer of cells was

detached in one piece and removed from the flask. Microglia remained attached to the bottom and were harvested by further trypsinization for 15–20 min. The purity of microglia was 98.5% as confirmed by CD11b, CX3CR1 and CD45 flow cytometric analysis (Fig. S1A). For astrocyte isolation [21], after 7–8 days culture, the flask was shaken at 180 rpm for 30 min to remove microglia. New medium was added into the flask followed by shaking at 240 rpm for 6 hours (hrs) to remove oligodendrocyte precursor cells. Astrocytes were detached by trypsin-EDTA, washed with PBS, and plated into two T75 culture flasks. Medium was changed every three days and astrocytes were harvested at 12–14 days after the first split. Astrocytes were then identified using IF staining of GFAP (Fig. S1B). For *in vitro* infections, a single dose of ZIKV (MOI of 1) was used.

RNA Isolation And Quantitative Real-time PCR (qRT-PCR)

RNA was isolated using Rneasy mini kit (Qiagen) according to the manufacturer's instructions. cDNA was synthesized using the iScript cDNA synthesis kit (Bio-Rad). The abundance of target genes was measured by qRT-PCR using a Bio-Rad CFX96 real-time PCR apparatus. SYBR Green Master Mix was from Bio-Rad, and TaqMan Universal Master Mix, including gene-specific probes and primers were from Integrated DNA Technologies (IDT). The relative level of gene expression was calculated using the $2^{-\Delta\Delta ct}$ method. The sequences of primers and probes are listed in Supplementary table 1.

Measurement Of Viral Burden

For measuring viral burden *in vivo*, mouse tissues were weighed and homogenized using a Tissue-Tearor (BioSpec). ZIKV RNA levels were determined by TaqMan quantitative reverse transcriptase PCR on the real-time PCR detection system (Bio-Rad). Virus burden was determined by interpolation onto an internal standard curve composed of serial 10-fold dilutions of a synthetic ZIKV RNA fragment. A previously published primer set was used to detect ZIKV RNA [22]. For measuring viral burden in infected cells *in vitro*, the relative level of gene expression was calculated based on C_t values using GAPDH as a housekeeping gene.

Lymphocytes Isolation And Purification

Lymphocytes were isolated according to our previously reported method [23]. Briefly, brains were cut into pieces and digested with 0.05% collagenase IV (Roche, Indianapolis, IN) at 37 °C for 30 min. Cell suspensions were passed through a 70-μm nylon cell strainer to yield single-cell suspensions. Lymphocytes were enriched by centrifugation (400 g) at room temperature for 30 min over a 30/70% discontinuous Percoll gradient (Sigma). Spleens were collected from mice and gently mashed in the RPMI-1640 medium through a cell strainer. Red blood cells were removed by using Red Cell Lysis Buffer (Sigma, St. Louis, MO). Cells were harvested by centrifugation (300 g, 10 min, 4 °C) and resuspended in RPMI-1640 medium plus 10% fetal bovine serum.

Flow Cytometry

Intracellular staining was performed with flow cytometry as in our previous report [23]. Briefly, for IL-22 and IL-17A detection, lymphocytes were cultured with rIL-23 (20 ng/ml) for 12 hrs. Brefeldin A solution (eBioscience) was added for the last 4 hrs of culture. For detecting IFN-γ and TNF-α in ZIKV-specific CD8 T cells, lymphocytes were incubated with ZIKV peptide $E_{294-302}$ (1 mg/mL, GenScript) in the presence of Brefeldin A solution for 5 hrs. Cells were then stained for anti-CD16/32 (Clone 2.4G2) and surface markers, fixed by using an IC fixation buffer, and followed by staining for intracellular cytokines (Thermo Fisher Scientific, Waltham, MA). Fixable viability dye, efluor 506 (Thermo Fisher Scientific), was also used to exclude dead cells. All samples were processed on an LSRII FACS Fortessa (Becton Dickinson, San Jose, CA) and analyzed using FlowJo software (TreeStar, Ashland, OR). The flow cytometry antibodies PE-Cy7-conjugated anti-CD3 (17A2), efluor450-conjugated anti-CD4 (GK1.5), APC-eFlour780-conjugated anti-CD8 (53 – 6.7), FITC- conjugated anti-NK1.1 (OK136), FITC- conjugated anti-TCR gamma/delta (GL3), PerCp-eFlour710-conjugated anti-TNF-α (MP6-XT22), APC-conjugated anti-IFN-γ (XMG1.2), APC-conjugated anti-CD45 (30-F11), Pacific Blue-conjugated anti-CD11b (M1/70), APC-conjugated anti-IL-17 (eBio17B7) and PE-conjugated anti-IL-22 (1H8PWSR) were purchased from Thermo Fisher Scientific. Purified anti-CD16/32 (2.4G2) and PE-conjugated anti-CX3CR1 (SA011F11) were purchased from Biolegend (San Diego, CA). CFSE dye was used for the cell proliferation assay.

ELISA

Tissue proteins were extracted using RIPA buffer (Cell Signaling Technology, Danvers, MA) and quantified using a BCA kit (Thermo Fisher Scientific). Mouse IL-22 ELISA kit was purchased from Thermo Fisher Scientific.

Immunofluorescence Staining And Confocal Microscopy

Mice were euthanized with CO_2 and perfused transcardially with cold PBS. Frontal cortices were collected and were immediately placed in 4% PFA in PBS at 4 °C overnight and then cryoprotected in a 30% sucrose solution in PBS for at least 24 hrs at 4 °C. Tissues were embedded in optimal cutting temperature compound (Sakura Finetek, Torrance, CA). Transverse sections (35 μm) were prepared on a cryostat (Leica CM 1900). The sections were kept in Hito floating section storage solution (Hitobiotec Corp) at -20 °C until they were stained for immunocytochemistry. For immunostaining, tissue sections were rinsed with PBS twice to remove the storage solution and blocked with 5% BSA and 0.3% Triton X-100 in PBS for 2 hrs at room temperature, followed by 48 hrs incubation with primary antibodies. After five washes with PBS, the sections were incubated with fluorophore-conjugated secondary antibodies at 4 °C overnight prior to section mounting. Confocal Z-stacks images were captured within the layer I-II of the cortex using a confocal microscope (Nikon A1). For each mouse, at least 3 fixed-frozen sections were included for each experiment, and at least 3 z-stacks images at 20 x, 40 x or 60 x magnification were taken. Thirty to fifty consecutive optical sections with 1 μm interval thickness at 40 x and 60 x magnification were

captured for each Z-stacks image. To process images, “Subtract Background” (50 pixels) was applied to remove the background and a threshold (50–225) was set to remove outliers. The analysis of positive areas and cell sizes were performed using Image J software. The rabbit-anti-Iba1 (Abcam, ab178846) and goat-anti-GFAP (Abcam, ab53554) antibodies were purchased from Abcam. The secondary antibodies, including goat anti-rabbit IgG (H + L) Alexa Fluor 488 and donkey anti-goat IgG (H + L) Alexa Fluor 555, were purchased from Thermo Fisher Scientific.

Western Blot Analysis

Total brain protein was homogenized in RIPA buffer including a 1% protease inhibitor cocktail (Sigma-Aldrich), and protein concentrations of the lysates were quantified using a BCA kit (Thermo Fisher Scientific). Five to twenty μg of proteins per sample were loaded onto a 12% Novex Tris-Glycine Gel and subsequently transferred to a PVDF membrane. The membrane was blotted with primary antibodies at 4 °C overnight. Antibody detection was accomplished using horseradish peroxidase conjugated secondary antibodies and visualized with ECL. Markers were used to identify the target protein band. As loading control, the expression of GAPDH was also measured. The signal intensity was quantified with Image Studio Lite. The primary antibodies anti-VE-cadherin, anti-ZO1, anti-Occluding, anti-Claudin 1 and anti-Claudin 3 were from Abcam. Anti-GAPDH was purchased from Cell Signaling Technology.

Statistical Analyses

Data were shown as mean ± SEM and analyzed using the two-tailed Student’s t-test when compared between two groups. One-way ANOVA was used for statistical analysis of more than two groups. A log-rank (Mantel-Cox) test was used for survival curve analysis. *, ** or *** means *P*-value < 0.05, < 0.01 or < 0.001, respectively. Statistical analyses were operated by GraphPad Prism software 7.0 (GraphPad Software Inc., San Diego, CA).

Results

ZIKV infection induced γδ T cell-derived IL-22

To investigate whether ZIKV infection can induce IL-22 expression, we infected 3-week-old IFNAR$^{-/-}$ mice with ZIKV as previously reported [24]. We observed that the infected mice started to lose weight at 4 days post infection (dpi) and all mice died at 6 dpi (Fig. S2A and B). Severe inflammatory infiltration appeared in the liver, lung and brain at 5 dpi, accompanied with increased expression of inflammatory genes, including IL-6, IL-1β, TNF-α and IFN-γ (Fig. S2C and D). We also found that IL-22 mRNA expression in the brain increased at 3 dpi and reached a peak at 5 dpi (Fig. 1A). On the contrary, splenic IL-22 mRNA was upregulated significantly at 3 dpi, and then returned to the baseline at 5 dpi. No considerable IL-22 upregulation was observed in the lung and liver following ZIKV infection (Fig. 1A). To define the source of IL-22 following infection, we isolated lymphocytes from the brain and spleen, and analyzed the IL-22-

expressing subpopulations. We found that IL-22 was mainly produced by γδ T cells, which also produced IL-17 (Fig. 1B). NK or conventional T cells had minimal or no detectable levels of IL-22 (data not shown). Consistently, the kinetic profile of IL-22^{+} γδ T cells in the brain and spleen showed the similar patterns as IL-22 transcript levels (Fig. 1B). We confirmed this finding using a WT (B6 background) mouse model by subcutaneously challenging one-day old neonatal mice with ZIKV (4×10^3 FFU). The infection of neonates resulted in an elevation of IL-22 expression in the spleen and brain at 2 and 13 dpi, respectively (Fig. 1C). Similarly, we showed that γδ T cells in these immunocompetent mice were the main producers of IL-22 and IL-17 (Fig. 1D). IL-22 protein levels were also increased in the brain, but not in the spleen at 13 dpi (Fig. 1E). Thus, our results indicated that ZIKV infection can induce IL-22 expression in γδ T cells.

IL-22 Deficiency Alleviated ZIKV-induced Neurological Disease In ZIKV Infection

To elucidate the role of IL-22 in ZIKV infection, we *s.c.* infected one-day old WT and IL-22$^{-/-}$ mice and monitored their bodyweight changes, survival rates and clinical manifestations. We found that ZIKV-infected IL-22$^{-/-}$ mice maintained significantly higher body weights starting at 8 dpi and continuing to the end of the observation period compared with that of infected WT mice (Fig. 2A). No significant difference in bodyweight was observed between WT and IL-22$^{-/-}$ mice without ZIKV infection (Fig. 2A). All IL-22$^{-/-}$ mice survived, while about 40% of the WT mice succumbed at 20 dpi (Fig. 2B). Consistently, the rate of paralysis for IL-22$^{-/-}$ mice was lower than that of WT mice (Fig. 2C). In the context of clinical manifestations, WT mice began to display staggered steps at 10 dpi, and around 60% of mice developed paralysis or seizure symptoms at 15 dpi. On the contrary, only 10% of IL-22$^{-/-}$ mice developed paralysis during the infection (Fig. 2D); neither seizure nor death was observed in the absence of IL-22. Full recovery was observed in about 90% of IL-22$^{-/-}$ mice by the end of the study, while none of the WT mice got full recovery at 20 dpi (Fig. 2D). To further confirm the detrimental role of IL-22, one-day old WT mice were infected with ZIKV, followed by recombinant IL-22 treatment every other day. We found that IL-22-treated mice exhibited reduced weight gain at 11 and 13 dpi compared with those of PBS-injected mice (Fig. 2E). Moreover, IL-22 treatment resulted in increased rates of paralysis at the same times (Fig. 2F). Collectively, we demonstrated that IL-22 plays a pathogenic role in ZIKV encephalitis.

IL-22 Deficiency Reduced Microglia Activation In ZIKV-infected Brain

Microglia cells are considered to be brain residential macrophages that are responsible for the clearance of invading pathogens and damaged neuronal cells [25]. However hyperactivation of microglia induces chronic inflammation and neurodegeneration [26]. ZIKV-infected microglia exhibit an activated phenotype, characterized by upregulation of several inflammatory cytokines and may also transmit virus to other target cells in the brain [9, 27]. To determine the role of IL-22 in microglial profile during ZIKV

infection, we analyzed the microglial phenotype in both IL-22$^{-/-}$ and WT neonatal mice. We found that ZIKV-infected IL-22$^{-/-}$ neonatal mice showed less number of activated microglia, as evidenced by decreased numbers of IBA-1^{+} cells in the cortex compared to WT control mice (Fig. 3A). Further analysis revealed that the amoeba-like microglia in IL-22$^{-/-}$ mice were smaller than those in WT mice, indicating there is reduced microglia activation in the absence of IL-22 (Fig. 3B). Similarly, the numbers of activated astrocytes, which were characterized as GFAP^{+}, were also lower in the cortex of IL-22$^{-/-}$ mice (Fig. 3A). We also examined the gene expression of inflammatory cytokines in the brain using qPCR. The mRNA levels of IFN-γ, as well as its inducible chemokines, CXCL9 and CXCL10, were not changed significantly. However, the level of brain TNF-α, which is the main cytokine produced by microglia [27, 28], was significantly decreased in IL-22$^{-/-}$ mice (Fig. S3). Therefore, these data suggested that IL-22-deficiency in ZIKV-infected neonatal mice resulted in reduced microglia activation and decreased pro-inflammatory TNF-α expression.

IL-22 played a dispensable role in ZIKV-induced glial cell activation in vitro

To determine whether IL-22 has a direct effect on glial cell activation and viral inoculation, mixed cortical cells were isolated from mouse pups and cultured *in vitro* for generating astrocytes and microglia (Fig. S1). Reactive astrocytes mainly display two polarizations, termed A1 and A2, which play neurotoxic and protective roles, respectively [18]. We found that ZIKV infection induced astrocyte activation and promoted an A1-prone phenotype. However, IL-22 did not show any effect on ZIKV-induced astrocyte activation (Fig. 4A). To determine whether IL-22 contributes to cell apoptosis and proliferation, we analyzed BCL2 and Ki67 transcript levels in ZIKV-infected astrocytes. Although ZIKV infection resulted in decreased cell survival and proliferation as evidenced by downregulation of BCL2 and Ki67 expression, no effect of IL-22 was observed on astrocytes *in vitro* (Fig. 4B). Finally, we measured viral loads in ZIKV-infected astrocytes in the presence of IL-22. Our data showed that ZIKV infected astrocytes efficiently, and IFN-γ significantly decreased viral burden at 24 hrs. However, either IL-22 alone or synergized with IFN-γ did not alter viral burdens (Fig. 4C). To further confirm our results, we infected human glial cell U-87MG with ZIKV, followed by rIL-22 treatment. Our results showed that IL-22 did not rescue cell death or promote cell proliferation (Fig. S4 A and B). The comparable transcript levels of CXCL10, CCL2 and BCL2, as well as viral loads were observed between control and rIL-22-treated groups (Fig. S4 C and D), indicating that IL-22 was dispensable for the growth, activation and viral infection of human glial cells. Microglia, as resident macrophages in the brain, have a high ability to secret inflammatory cytokines (e.g. TNF-α), which induce astrocyte A1 polarization and lead to neuron death [18]. Our qPCR data showed that ZIKV-infected mouse primary microglia increased the expression of several inflammatory cytokine genes, including TNF-α, IL-1β, CXCL2 and CCL2 (Fig. 4D). Arginase-1 (Arg-1) can compete with nitric oxide synthase in the brain, playing a neuroprotective role [29]. We found reduced Arg-1 expression in microglia following ZIKV infection, suggesting to us that ZIKV may cause damage in the brain through inhibiting neuroprotective factors. In addition, ZIKV-infected microglia downregulated anti-apoptotic gene BCL2 expression, indicating that ZIKV infection may promote glial cell apoptosis (Fig. 4D). Although microglia were infected by ZIKV, IL-22 did not contribute to this infection or cell activation, as evidenced by similar

levels of viral loads and comparable gene expression of activation markers following IL-22 supplementation *in vitro* (Fig. 4D). Since human Th17 cells are known to promote BBB disruption and CNS inflammation [17], we measured several tight junction proteins, including ZO-1, VE-cadherin, Occludin, Claudin-1, and Claudin-3 in the brain of both ZIKV-infected WT and IL-22$^{-/-}$ mice. Similar levels of these tight junction proteins were detected, implying that IL-22 may not disrupt the BBB during ZIKV infection (Fig. S5). Therefore, our data demonstrated that ZIKV infection induced neurotoxic reactive astrocytes and activated microglia, leading to brain inflammation, and that IL-22 was dispensable for glial cell activation, polarization and viral clearance *in vitro*.

IL-22 Hindered Anti-ZIKV CD8$^+$ T Cell Responses

Although immune cells do not express IL-22 receptor, IL-22 can regulate T cell responses in both viral and parasitic infection, probably via indirect ways [14]. The adaptive immune response, especially the anti-ZIKV cytotoxic CD8 T cell response, has been demonstrated to play a protective role against ZIKV infection [30, 31]. However, excessive CD8$^+$ T cell infiltration in the brain can cause paralysis in mice with ZIKV infection [32]. Here, we speculated that the absence of IL-22 resulted in more robust CD8$^+$ T cell responses which efficiently controlled ZIKV infection. To test this hypothesis, we *s.c.* infected one-day old WT and IL-22$^{-/-}$ mice, and interrogated viral burdens and anti-ZIKV CD8$^+$ T cell responses. We found that tissue viral load spiked at 13 dpi in WT mice, with much higher levels in the brain compared with those in the spleen (Fig. 5A and B). Importantly, IL-22$^{-/-}$ mice displayed significantly lower viral loads in both the spleen and brain at the peak of viral infection (13 dpi), but not at other time-points including 2, 7 and 20 dpi (Fig. 5A and B). IL-22$^{-/-}$ mice displayed more effective anti-ZIKV CD8$^+$ T cell responses, as evidenced by increased numbers of IFN-γ$^+$CD8$^+$ T cells (Fig. 5C). However, comparable numbers of infiltrated lymphocytes and IFN-γ$^+$CD8$^+$ T cells were found in the brains of WT and IL-22$^{-/-}$ mice at 13 dpi (Fig. 5D). These results may indicate that IL-22 deficiency promoted effector functions of antiviral CD8$^+$ T cells, without increasing inflammatory infiltration to the brain. Consistently, exogenous IL-22 treatment increased brain viral loads and impaired anti-ZIKV CD8$^+$ T cell responses in both the spleen and brain (Fig. 5E and F). We also confirmed our finding using a three-week old immunocompetent mouse model. Again, IL-22-deficiency resulted in increased cytokine-producing CD8$^+$ T cells in the spleen at 7 dpi (Fig. S6). Collectively, our findings suggested that IL-22 dampens anti-ZIKV T cell responses in the periphery and exacerbates viral infection in the brain, leading to profound cerebral inflammation and animal paralysis and death.

Discussion

The roles of IL-22 in various diseases are diverse. In mucosal disorders, IL-22 plays a protective role by preserving epithelial integrity [33, 34], promoting antibacterial peptides and proteins [35], and inducing mucins [36, 37]. However, IL-22 is pathogenic in some inflammatory settings, such as psoriasis [38], allergic airway inflammation [39] and collagen-induced arthritis [40]. The role of IL-22 in viral infection is

enigmatic. Our previous research indicated that IL-22 contributes to antiviral immune responses and determines viral clearance in LCMV infection [14]. In this study with ZIKV infection, we found that deficiency of IL-22 resulted in decreased viral loads, alleviated clinical manifestations, and increased survival rates in neonatal mice (Fig. 1–3). Our *in vitro* results showed that ZIKV infection promoted the polarization of neurotoxic reactive astrocytes and the activation of microglia, which may induce neuroinflammation in the brain [18]. Although IL-22 did not directly exert its effects on brain glial cells *in vitro*, the absence of IL-22 led to reduced glial cell activation *in vivo* (Fig. 4). More importantly, IL-22$^{-/-}$ mice elicited qualitatively better ZIKV-specific T cell responses compared with those in WT mice. Therefore, our results demonstrated a pathogenic role of IL-22 in ZIKV encephalitis of neonatal mice.

Upon viral infection, IL-22 induction is organ-specific. NK and NKT cells can produce IL-22 in response to murine cytomegalovirus and influenza virus infection [41–43]. Intrahepatic γδ T cells are also the source of IL-22 in hepatitis B virus-infected patients [44]. We have previously reported that intrahepatic γδ T cells are the main immune cells to produce IL-22 by IL-23 stimulation in an LCMV-infected mouse model [14]. Similarly, we found in this study that γδ T cells were the main source of IL-22 in the spleen and brain in both IFNAR$^{-/-}$ and WT neonatal mouse models (Fig. 1). The peak of IL-22 expression in the spleen was as early as 2 dpi, while the time-point for peak expression of IL-22 in the brain was delayed. Since ZIKV initially infected lymphoid organs and subsequently invaded the CNS [24], this dynamic pattern of IL-22 suggests that IL-22 might be driven by the virus or virus-induced innate immune responses. Indeed, ZIKV infection induced high levels of brain inflammatory cytokines, including IL-1β (Fig. S1D), which may facilitate the expression of IL-22 from γδ T cells [45]. In addition, high level of IL-6 in the brain, but not in the liver and lung, also suggest that IL-6 may be required for IL-22 production perhaps through the induction of downstream IL-21[46].

Both WNV and ZIKV belong to the flaviviridae family and cause severe encephalitis, yet the IL-22-mediated immune regulation seems to be different in the CNS. It has been reported that IL-22$^{-/-}$ mice were resistant to lethal WNV infection due to reduced inflammatory infiltration and decreased viral load in the CNS [15]. We found that in IL-22$^{-/-}$ mice, infection of both WNV and ZIKV led to alleviated clinical manifestations (Fig. 2) with decreased viral load and elevated pro-inflammatory TNF-α expression in the brain (Fig. 5A and S3) [15], whereas recombinant IL-22 cytokine treatment *in vivo* restored the detrimental role of IL-22 (Fig. 2E). Interestingly, there were several distinct aspects between WNV and ZIKV infection in IL-22$^{-/-}$ mice. First, IL-22 was critical for virus-carrying neutrophil migration through the blood brain barrier, leading to severe WNV infection in the brain [15]; however, ZIKV-infected IL-22$^{-/-}$ mice showed similar levels of lymphocyte infiltration, chemokine expression and tight junction proteins in the brain (Fig. 5D, S3 and S5). It is reported that neutrophil migration from the blood into the brain was strikingly reduced in WNV-infected IL-22$^{-/-}$ mice [15]. Although we observed neutrophil infiltration in the brain during ZIKV infection, the absence of IL-22 did not change the number of infiltrated neutrophil (data not shown). These results indicated that the inflammatory infiltration and BBB may not be the main reason for the alleviated clinical manifestations in IL-22$^{-/-}$ mice during ZIKV infection. Secondly, IL-22 deficiency did not contribute to the anti-WNV immunity in the periphery [15], but actually resulted in more vigorous

ZIKV-specific $CD8^+$ T cell responses in the spleen (Fig. 5C and S6). In line with the recent findings that $CD8^+$ T cells protected against ZIKV infection in the CNS [31, 47, 48], our study suggests that IL-22 may contribute to ZIKV encephalitis pathogenesis by modulating periphery $CD8^+$ T cell responses. Additional evidence is that IL-22 deficiency did not influence WNV burdens in the spleen [15]; however, IL-$22^{-/-}$ mice had lower viral loads in the spleen following ZIKV infection (Fig. 5A). The possible reasons for these discrepancies could be related to diversity of the two viruses and differences of the animal models.

ZIKV can target several types of glial cells, including astrocytes and microglia, leading to intracranial viral spreading, brain inflammation and fetal congenital malformations [2, 9, 10]. Microglia-derived TNF-α plays a critical role as an inflammatory mediator and can further activate microglia through an autocrine manner [28]. Neutralization of TNF-α or depletion of microglia prevents memory impairment in ZIKV-infected mice [49], indicating that microglia and TNF-α play detrimental roles in ZIKV infection. We showed in this study that ZIKV infection caused the activation of microglia, as evidenced by the formation of amoeba-like shapes (Fig. 3B) [25]. We also found that IL-22 deficiency resulted in reduced microglia numbers as well as cell activation (Fig. 3A and B). In addition, decreased TNF-α expression was observed in the brain of IL-$22^{-/-}$ mice (Fig. S3). Our *in vivo* results suggested that IL-22 may contribute to glial cell activation and induce brain inflammation, leading to cerebral pathogenesis. In addition to microglia, astrocytes are considered the initial target of ZIKV infection immediately following viral inoculation of newborn mice [10]. A recent study explored whether activated microglia can produce inflammatory factors (e.g. TNF-α, IL-1β and complement C1q) to induce astrocyte polarization into neurotoxic A1 astrocytes, which secret neurotoxins and rapidly degenerate neurons and mature differentiated oligodendrocytes [18]. Our finding that the absence of IL-22 resulted in decreased astrocyte activation (Fig. 3A), leads us to examine whether ZIKV infection promotes neurotoxic A1 polarization. Our *in vitro* data comprehensively demonstrated the pan-reactive and A1-prone phenotype of astrocytes during ZIKV infection, although some A2 typical gene transcripts were also upregulated (Fig. 4A). Our data indicated that ZIKV not only infects astrocytes for replication, but also directly induces astrocytes to shape a neurotoxic phenotype. Moreover, ZIKV-activated microglia may also facilitate A1 polarization through producing TNF-α and IL-1β, which were highly expressed in the brain following ZIKV infection (Fig. S1D).

Whether IL-22 can directly affect glial cells and regulate cell function is not entirely clear. IL-22 receptor was detected in human astrocytes of both healthy controls and multiple sclerosis patients, and IL-22 treatment reduced TNF-α-induced apoptosis of astrocytes [16]. In addition, exogenous IL-22 also promoted the proliferation of human glial cells accompanied by an anti-apoptotic effect [50]. To our surprise, such effects of IL-22 on astrocytes or microglia were not observed in our study using a human glial cell line, and mouse primary astrocytes or microglia (Fig. 4 and S4). Although ZIKV infection significantly inhibited cell growth and elevated inflammatory gene expression, supplementing with IL-22 showed a dispensable role in cell proliferation and activation. Moreover, neither IL-22 alone nor synergizing with IFN-γ contributed to ZIKV replication in astrocytes and microglia (Fig. 4C). In addition, we were unable to detect IL-22R1 transcript in mouse primary astrocytes and microglia by qPCR (data not

shown). These data suggest that IL-22 may not be capable of directly regulating glial cell function in the brain; instead, IL-22 appears to dampen antiviral T cell responses and delay viral clearance in the periphery, probably leading to more ZIKV invasion of the brain, increased glial cell activation and increased disease severity. However, we could not exclude the possibility that IL-22R1 may be inducible and upregulated by the inflammatory cytokines in the brain due to the disease status. Additionally, IL-22 may need a synergetic mechanism with critical cytokines, such as IFN-λ, to amplify the downstream signals and execute the function [51]. Although the reason for the discrepancies in ours and others' studies is not known at present, further investigation is needed to clarify the unique role of IL-22 in the CNS among distinct disease animal models.

Conclusions

Taken together, our studies demonstrated that ZIKV infection promoted microglial activation and facilitated an A1-prone phenotype of neurotoxic astrocytes, whereas the absence of IL-22 resulted in reduced glial cell activation and alleviated clinical symptoms in a ZIKV encephalitis neonatal mouse model. Importantly, IL-22 dampened anti-ZIKV T cell responses and delayed viral clearance, suggesting that the neutralization of IL-22 may be a potential therapeutic against ZIKV encephalitis.

Abbreviations

ZIKV
Zika virus
WT
wild-type
dpi
days post infection
LCMV
lymphocytic choriomeningitis virus
WNV
West Nile virus
BBB
Blood brain barrier
CNS
central nervous system
FFU
fluorescent focus units
s.c.
subcutaneous
hours
hrs

Declarations

Ethics statement

This study was carried out in accordance with the recommendations in the Guide for the Care and Use of Laboratory Animals of the National Institutes of Health. All animal procedures were performed in compliance with the Institutional Animal Care and Use Committee (protocol # 1606029) at the University of Texas Medical Branch (UTMB) in Galveston, TX. All of efforts were exerted to minimize the suffering of experimental animals.

Consent for publication

Not applicable.

Competing interests

The authors declare that they have no conflict of interest.

Availability of data and materials

All data generated or analysed during this study are included in this published article and its supplementary information files.

Funding

This work was supported in part by grants from the NIH (EY028773 to JC and JS; AI132674 to LS). TG was the recipient of summer internships from an NIAID T35 training grant (AI078878, PI: LS).

Author contributions

Conceived and designed the experiments: YL, PY, LS and JS. Performed the experiments: YL, PY, WR, HW, TG and JL. Analyzed the data: YL, PY, HW, XW and JS. Contributed reagents/materials/analysis tools: ZJ, EA, HH, LS. Wrote the paper: YL, PY, EA, LS, JC and JS.

Acknowledgements

We thank Dr. Sherry Haller and Dr. Shaojun Tang for assistance with manuscript preparation. The authors wish to express gratitude to other members of the UTMB Joint Immunology Working Group (Drs. Cong, Stephens, Rajsbaum, Hu, and their trainees) for many helpful discussions.

References

1. Driggers RW, Ho CY, Korhonen EM, Kuivanen S, Jaaskelainen AJ, Smura T, et al. Zika Virus Infection with Prolonged Maternal Viremia and Fetal Brain Abnormalities. N Engl J Med. 2016;347:2142–51.
2. Mlakar J, Korva M, Tul N, Popovic M, Poljsak-Prijatelj M, Mraz J, et al. Zika Virus Associated with Microcephaly. N Engl J Med. 2016;374:951–8.
3. Lazear HM, Diamond MS. Zika Virus: New Clinical Syndromes and Its Emergence in the Western Hemisphere. J Virol. 2016;90:4864–75.
4. Petersen LR, Jamieson DJ, Powers AM, Honein MA. Zika Virus. N Engl J Med. 2016;375:294–95.
5. Barbi L, Coelho AVC, Alencar LCA, Crovella S. Prevalence of Guillain-Barre syndrome among Zika virus infected cases: a systematic review and meta-analysis. Braz J Infect Dis. 2018;22:137–41.
6. Rubin EJ, Greene MF, Baden LR. Zika Virus and Microcephaly. N Engl J Med. 2016;374:984–5.
7. Tang H, Hammack C, Ogden SC, Wen Z, Qian X, Li Y, et al. Zika Virus Infects Human Cortical Neural Progenitors and Attenuates Their Growth. Cell Stem Cell. 2016;18:587–90.
8. Li H, Saucedo-Cuevas L, Yuan L, Ross D, Johansen A, Sands D, et al. Zika Virus Protease Cleavage of Host Protein Septin-2 Mediates Mitotic Defects in Neural Progenitors. Neuron. 2019;101:1089-98 e4.
9. Lum FM, Low DK, Fan Y, Tan JJ, Lee B, Chan JK, et al. Zika Virus Infects Human Fetal Brain Microglia and Induces Inflammation. Clin Infect Dis. 2017;64:914–20.
10. van den Pol AN, Mao G, Yang Y, Ornaghi S, Davis JN. Zika Virus Targeting in the Developing Brain. J Neurosci. 2017;37:2161–75.
11. Stefanik M, Formanova P, Bily T, Vancova M, Eyer L, Palus M, et al. Characterisation of Zika virus infection in primary human astrocytes. BMC Neurosci. 2018;19:5.
12. Dudakov JA, Hanash AM, van den Brink MR. Interleukin-22: immunobiology and pathology. Annu Rev Immunol. 2015;33:747–85.
13. Ouyang W, O'Garra A. IL-10 Family Cytokines IL-10 and IL-22: from Basic Science to Clinical Translation. Immunity. 2019;50:871–91.
14. Yi P, Liang Y, Yuan DMK, Jie Z, Kwota Z, Chen Y, et al. A tightly regulated IL-22 response maintains immune functions and homeostasis in systemic viral infection. Sci Rep. 2017;7:3857.
15. Wang P, Bai F, Zenewicz LA, Dai J, Gate D, Cheng G, et al. IL-22 signaling contributes to West Nile encephalitis pathogenesis. PLoS One. 2012;7:e44153.
16. Perriard G, Mathias A, Enz L, Canales M, Schluep M, Gentner M, et al. Interleukin-22 is increased in multiple sclerosis patients and targets astrocytes. J Neuroinflammation. 2015;12:119.
17. Kebir H, Kreymborg K, Ifergan I, Dodelet-Devillers A, Cayrol R, Bernard M, et al. Human TH17 lymphocytes promote blood-brain barrier disruption and central nervous system inflammation. Nat Med. 2007;13:1173–5.
18. Liddelow SA, Guttenplan KA, Clarke LE, Bennett FC, Bohlen CJ, Schirmer L, et al. Neurotoxic reactive astrocytes are induced by activated microglia. Nature. 2017;541:481–87.

19. Manangeeswaran M, Ireland DD, Verthelyi D. Zika (PRVABC59) Infection Is Associated with T cell Infiltration and Neurodegeneration in CNS of Immunocompetent Neonatal C57Bl/6 Mice. PLoS Pathog. 2016;12:e1006004.
20. Saura J, Tusell JM, Serratosa J. High-yield isolation of murine microglia by mild trypsinization. Glia. 2003;44:183–9.
21. Schildge S, Bohrer C, Beck K, Schachtrup C. Isolation and culture of mouse cortical astrocytes. J Vis Exp. 2013:50079.
22. Chen J, Liang Y, Yi P, Xu L, Hawkins HK, Rossi SL, et al. Outcomes of Congenital Zika Disease Depend on Timing of Infection and Maternal-Fetal Interferon Action. Cell Rep. 2017;21:1588–99.
23. Liang Y, Yi P, Yuan DMK, Jie Z, Kwota Z, Soong L, et al. IL-33 induces immunosuppressive neutrophils via a type 2 innate lymphoid cell/IL-13/STAT6 axis and protects the liver against injury in LCMV infection-induced viral hepatitis. Cell Mol Immunol. 2019;16:126–37.
24. Rossi SL, Tesh RB, Azar SR, Muruato AE, Hanley KA, Auguste AJ, et al. Characterization of a Novel Murine Model to Study Zika Virus. Am J Trop Med Hyg. 2016;94:1362.
25. Chen Z, Zhong D, Li G. The role of microglia in viral encephalitis: a review. J Neuroinflammation. 2019;16:76.
26. Alamer E, Zhong C, Liu Z, Niu Q, Long F, Guo L, et al. Epigenetic Suppression of HIV in Myeloid Cells by the BRD4-Selective Small Molecule Modulator ZL0580. J Virol. 2020;94:e01880-19.
27. Diop F, Vial T, Ferraris P, Wichit S, Bengue M, Hamel R, et al. Zika virus infection modulates the metabolomic profile of microglial cells. PLoS One. 2018;13:e0206093.
28. Kuno R, Wang J, Kawanokuchi J, Takeuchi H, Mizuno T, Suzumura A. Autocrine activation of microglia by tumor necrosis factor-alpha. J Neuroimmunol. 2005;162:89–96.
29. Madan S, Kron B, Jin Z, Al Shamy G, Campeau PM, Sun Q, et al. Arginase overexpression in neurons and its effect on traumatic brain injury. Mol Genet Metab. 2018;125:112–17.
30. Pardy RD, Rajah MM, Condotta SA, Taylor NG, Sagan SM, Richer MJ. Analysis of the T Cell Response to Zika Virus and Identification of a Novel CD8 + T Cell Epitope in Immunocompetent Mice. PLoS Pathog. 2017;13:e1006184.
31. Huang H, Li S, Zhang Y, Han X, Jia B, Liu H, et al. CD8(+) T Cell Immune Response in Immunocompetent Mice during Zika Virus Infection. J Virol. 2017;91:e00900-17.
32. Jurado KA, Yockey LJ, Wong PW, Lee S, Huttner AJ, Iwasaki A. Antiviral CD8 T cells induce Zika-virus-associated paralysis in mice. Nat Microbiol. 2018;3:141–47.
33. Lo BC, Shin SB, Canals Hernaez D, Refaeli I, Yu HB, Goebeler V, et al. IL-22 Preserves Gut Epithelial Integrity and Promotes Disease Remission during Chronic Salmonella Infection. J Immunol. 2019;202:956–65.
34. Schreiber F, Arasteh JM, Lawley TD. Pathogen Resistance Mediated by IL-22 Signaling at the Epithelial-Microbiota Interface. J Mol Biol. 2015;427:3676–82.

35. Moyat M, Bouzourene H, Ouyang W, Iovanna J, Renauld JC, Velin D. IL-22-induced antimicrobial peptides are key determinants of mucosal vaccine-induced protection against H. pylori in mice. Mucosal Immunol. 2017;10:271–81.
36. Sugimoto K, Ogawa A, Mizoguchi E, Shimomura Y, Andoh A, Bhan AK, et al. IL-22 ameliorates intestinal inflammation in a mouse model of ulcerative colitis. J Clin Invest. 2008;118:534–44.
37. Aujla SJ, Chan YR, Zheng M, Fei M, Askew DJ, Pociask DA, et al. IL-22 mediates mucosal host defense against Gram-negative bacterial pneumonia. Nat Med. 2008;14:275–81.
38. Zheng Y, Danilenko DM, Valdez P, Kasman I, Eastham-Anderson J, Wu J, et al. Interleukin-22, a T(H)17 cytokine, mediates IL-23-induced dermal inflammation and acanthosis. Nature. 2007;445:648–51.
39. Leyva-Castillo JM, Yoon J, Geha RS. IL-22 promotes allergic airway inflammation in epicutaneously sensitized mice. J Allergy Clin Immunol. 2019;143:619–30.
40. Geboes L, Dumoutier L, Kelchtermans H, Schurgers E, Mitera T, Renauld JC, et al. Proinflammatory role of the Th17 cytokine interleukin-22 in collagen-induced arthritis in C57BL/6 mice. Arthritis Rheum. 2009;60:390–5.
41. Guo H, Topham DJ. Interleukin-22 (IL-22) production by pulmonary Natural Killer cells and the potential role of IL-22 during primary influenza virus infection. J Virol. 2010;84:7750–9.
42. Paget C, Ivanov S, Fontaine J, Renneson J, Blanc F, Pichavant M, et al. Interleukin-22 is produced by invariant natural killer T lymphocytes during influenza A virus infection: potential role in protection against lung epithelial damages. J Biol Chem. 2012;287:8816–29.
43. Stacey MA, Marsden M, Pham NT, Clare S, Dolton G, Stack G, et al. Neutrophils recruited by IL-22 in peripheral tissues function as TRAIL-dependent antiviral effectors against MCMV. Cell Host Microbe. 2014;15:471–83.
44. Zhao J, Zhang Z, Luan Y, Zou Z, Sun Y, Li Y, et al. Pathological functions of interleukin-22 in chronic liver inflammation and fibrosis with hepatitis B virus infection by promoting T helper 17 cell recruitment. Hepatology. 2014;59:1331–42.
45. Malik S, Want MY, Awasthi A. The Emerging Roles of Gamma-Delta T Cells in Tissue Inflammation in Experimental Autoimmune Encephalomyelitis. Front Immunol. 2016;7:14.
46. Zhou L, Ivanov II, Spolski R, Min R, Shenderov K, Egawa T, et al. IL-6 programs T(H)-17 cell differentiation by promoting sequential engagement of the IL-21 and IL-23 pathways. Nat Immunol. 2007;8:967–74.
47. Elong Ngono A, Vizcarra EA, Tang WW, Sheets N, Joo Y, Kim K, et al. Mapping and Role of the CD8 + T Cell Response During Primary Zika Virus Infection in Mice. Cell Host Microbe. 2017;21:35–46.
48. Hassert M, Harris MG, Brien JD, Pinto AK. Identification of Protective CD8 T Cell Responses in a Mouse Model of Zika Virus Infection. Front Immunol. 2019;10:1678.
49. Figueiredo CP, Barros-Aragao FGQ, Neris RLS, Frost PS, Soares C, Souza INO, et al. Zika virus replicates in adult human brain tissue and impairs synapses and memory in mice. Nat Commun. 2019;10:3890.

50. Akil H, Abbaci A, Lalloue F, Bessette B, Costes LM, Domballe L, et al. IL22/IL-22R pathway induces cell survival in human glioblastoma cells. PLoS One. 2015;10:e0119872.

51. Hernandez PP, Mahlakoiv T, Yang I, Schwierzeck V, Nguyen N, Guendel F, et al. Interferon-lambda and interleukin 22 act synergistically for the induction of interferon-stimulated genes and control of rotavirus infection. Nat Immunol. 2015;16:698–707.

Figures

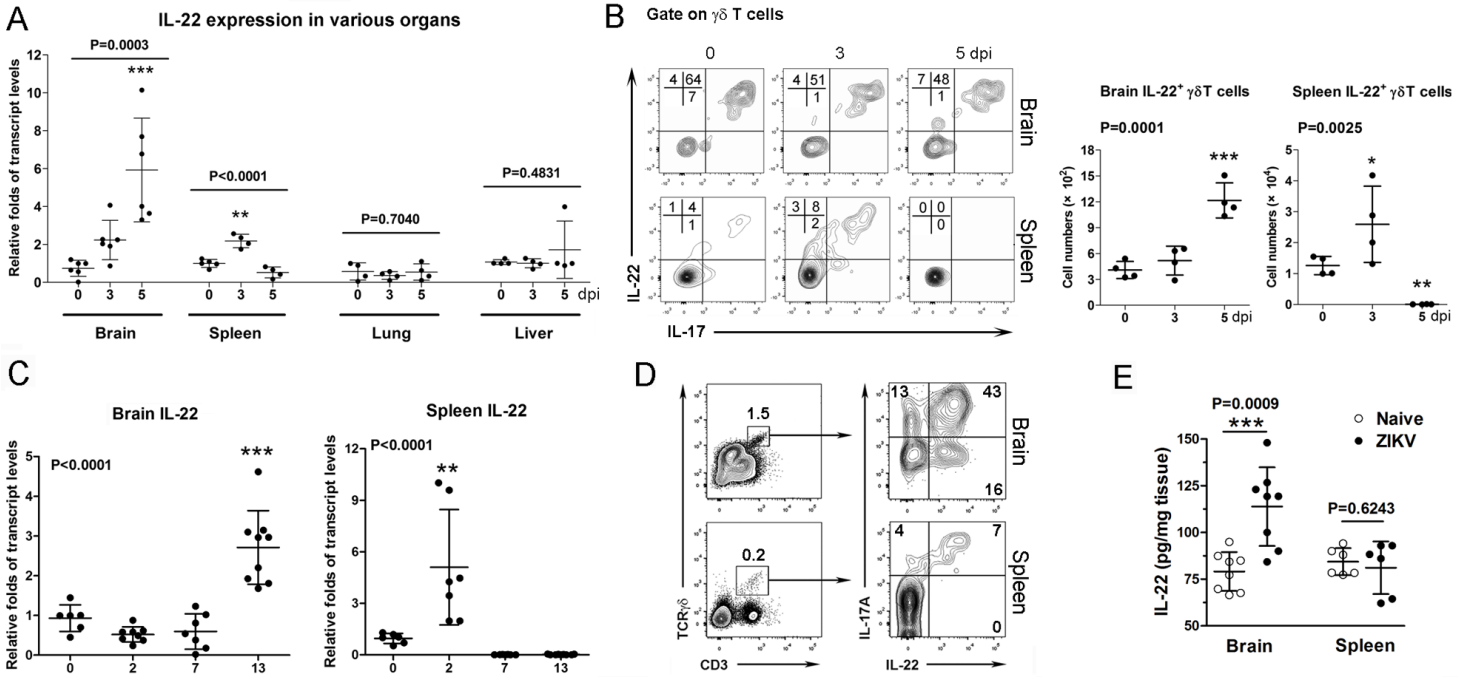


Figure 1

ZIKV infection induces IL-22 expression. (A) Transcript levels of IL-22 were measured in various organs of ZIKV-infected IFNAR-/- mice. (B) ▯▯17 and ▯▯22 were analyzed in the brain and spleen of ZIKV-infected IFNAR-/- mice. (C) Neonatal B6 mice were s.c. infected with ZIKV, and viral loads were measured in the brain and spleen. (D) ▯▯17 and ▯▯22 were analyzed in the brain and spleen of ZIKV-infected neonatal B6 mice at 13 dpi. (E) IL-22 protein levels were quantified in the brain and spleen at 13 dpi. All experiments were repeated twice independently. A two-tailed Student's t-test was used to compare the two groups. One-way ANOVA was used to compare more than two groups. * P<0.05, ** P<0.01, *** P<0.001.

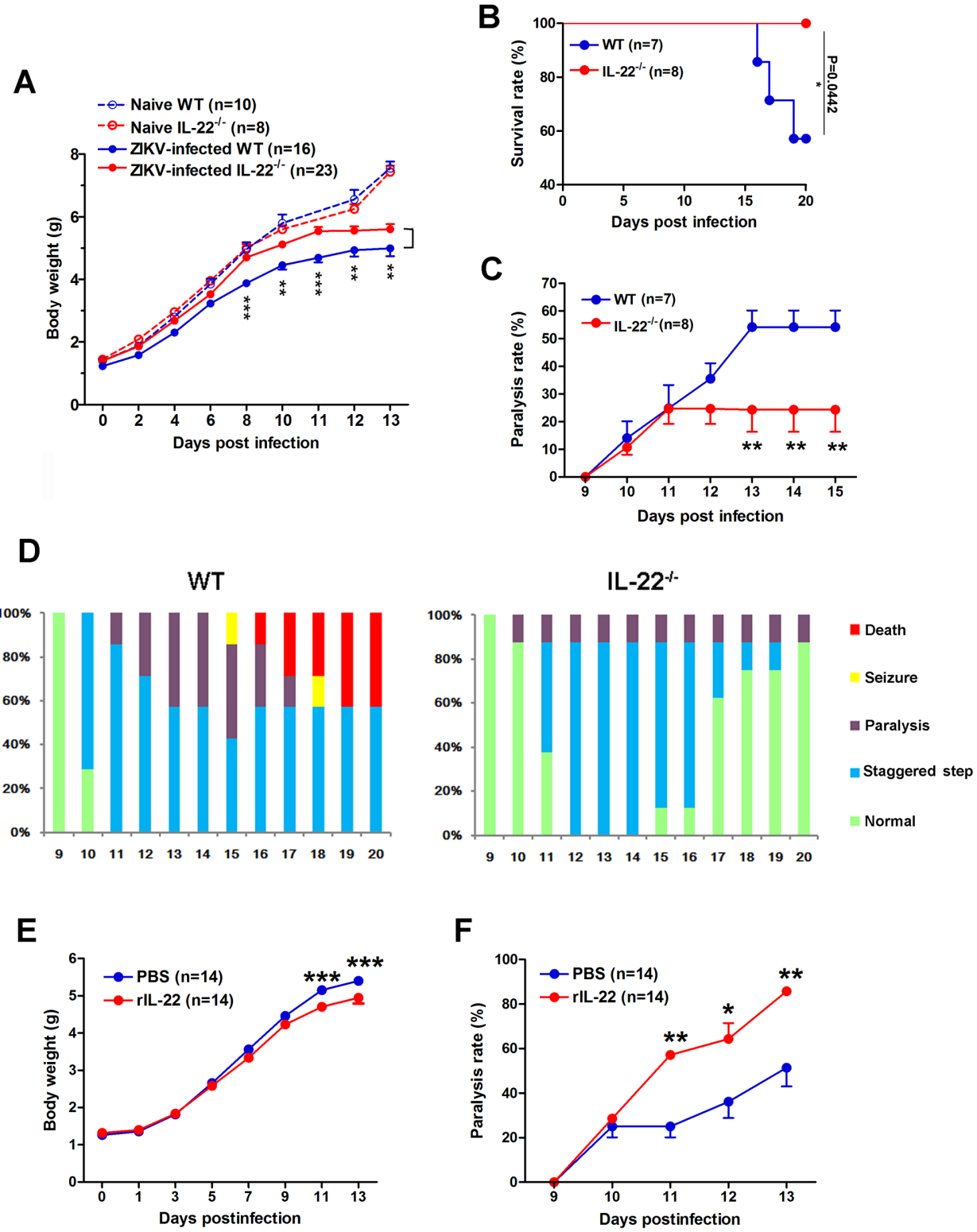


Figure 2

IL-22 deficiency leads to attenuated clinical symptoms in ZIKV-infected neonatal mice. Neonatal WT and IL-22-/- mice were s.c. infected with ZIKV. (A) Body weight, (B) survival rates, (C) paralysis rates and (D) clinical manifestations were monitored. (E) Neonatal WT mice were s.c. infected with ZIKV, followed by recombinant IL-22 treatment (1 μg in 5 μL, s.c.) every other day. Bodyweight and (F) paralysis rates were recorded. The numbers of samples (n) were shown in the figures. All experiments were repeated twice

independently. A two-tailed Student's t-test was used to compare the two groups. One-way ANOVA was used to compare more than two groups. Log-rank (Mantel-Cox) test was used for survival curve analysis. * P<0.05, ** P<0.01, *** P<0.001.

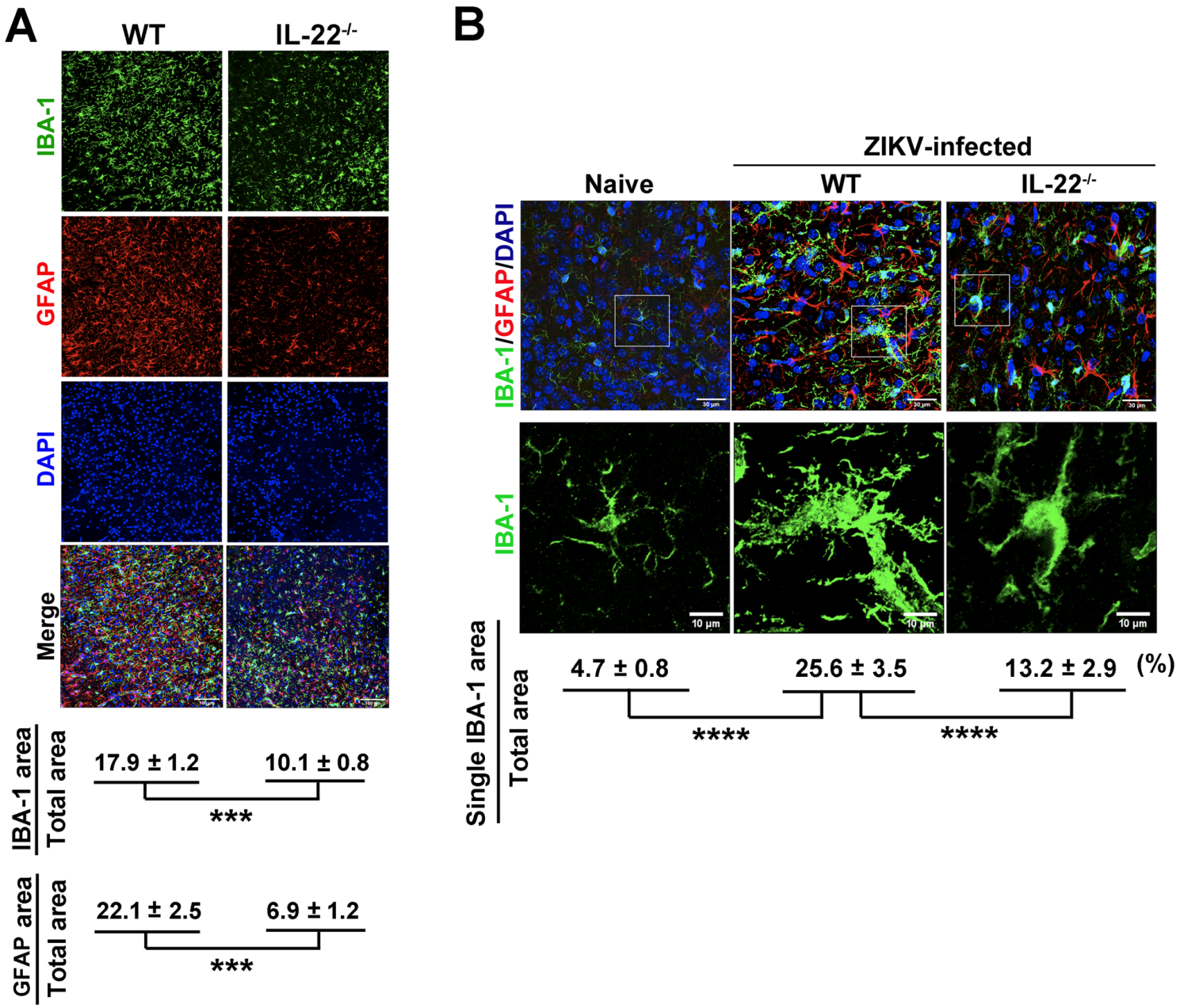


Figure 3

IL-22 deficiency results in decreased microglia and astrocyte activation. Neonatal WT and IL-22-/- mice (4-5/group) were s.c. infected with ZIKV and sacrificed at 13 dpi. (A) Immunostaining of IBA-1 (microglia cells) and GFAP (astrocytes) in the cerebral cortex. Scale bars, 25 μm. (B) IBA-1 staining area of single microglia cells in the cerebral cortex. The lower images represent the rectangular area of view in upper images. Scale bars for upper and lower images were 30 and 10 μm, respectively. The areas of staining were quantified by Image J software. At least six sections from each of four to five brains per group were examined. All experiments were repeated twice independently. Data are shown as means ± SEM. A two-

tailed Student's t-test was used to compare the two groups in panel A. One-way ANOVA was used to compare three groups in panel B. *** P<0.001, **** P<0.0001.

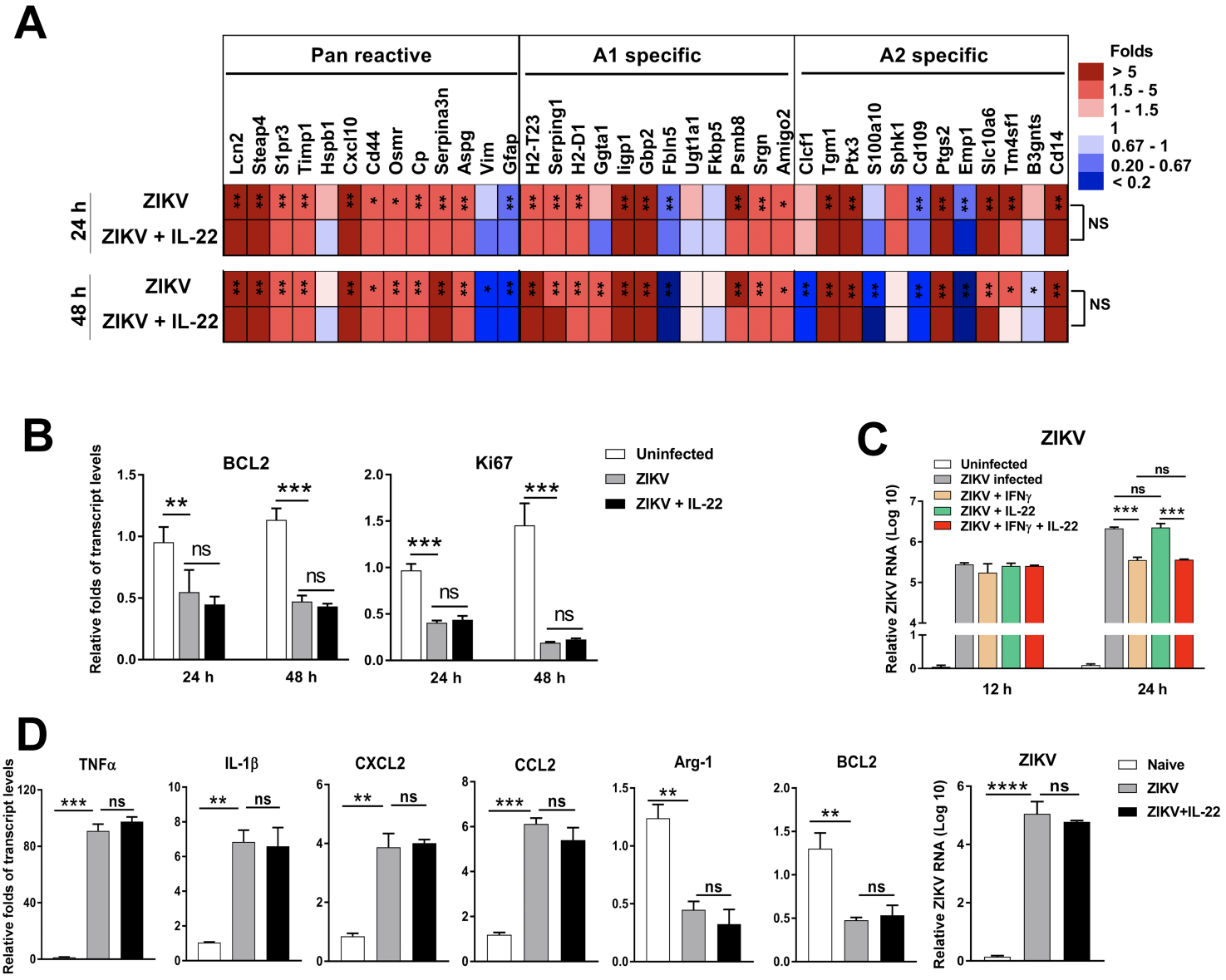


Figure 4

ZIKV induces A1-prone astrocytes, but IL-22 plays a dispensable role in vitro. (A) Mouse primary astrocytes were infected by ZIKV with recombinant IL-22 (200 ng/mL) added or omitted in vitro. Uninfected cells were used as a control. Cells were harvested at 24 and 48 hrs, followed by qRT-PCR analysis for astrocyte activation and (B) apoptosis/proliferation markers. In panel A, the fold changes of infected groups were normalized to those of uninfected controls. The asterisks in ZIKV group indicated the results of statistical analysis between ZIKV and control groups. No significant difference was found for any marker between ZIKV and ZIKV+IL-22 groups. (C) Mouse primary astrocytes were infected by ZIKV with or without recombinant IL-22 (200 ng/mL) and IFN-β (100 ng/mL) in vitro. Viral loads were measured at 12 and 24 hrs. (D) Mouse primary microglia cells were infected by ZIKV with recombinant IL-22 (200 ng/mL) added or omitted in vitro. Transcript levels of inflammatory cytokines and anti-apoptotic marker as well as viral burdens were examined by qPCR. All experiments were repeated twice

independently. Data are shown as means ± SEM. Each group contains at least three samples, and One-way ANOVA was used to compare three groups. * P<0.05, ** P<0.01, *** P<0.001, **** P<0.0001, NS, not significant.

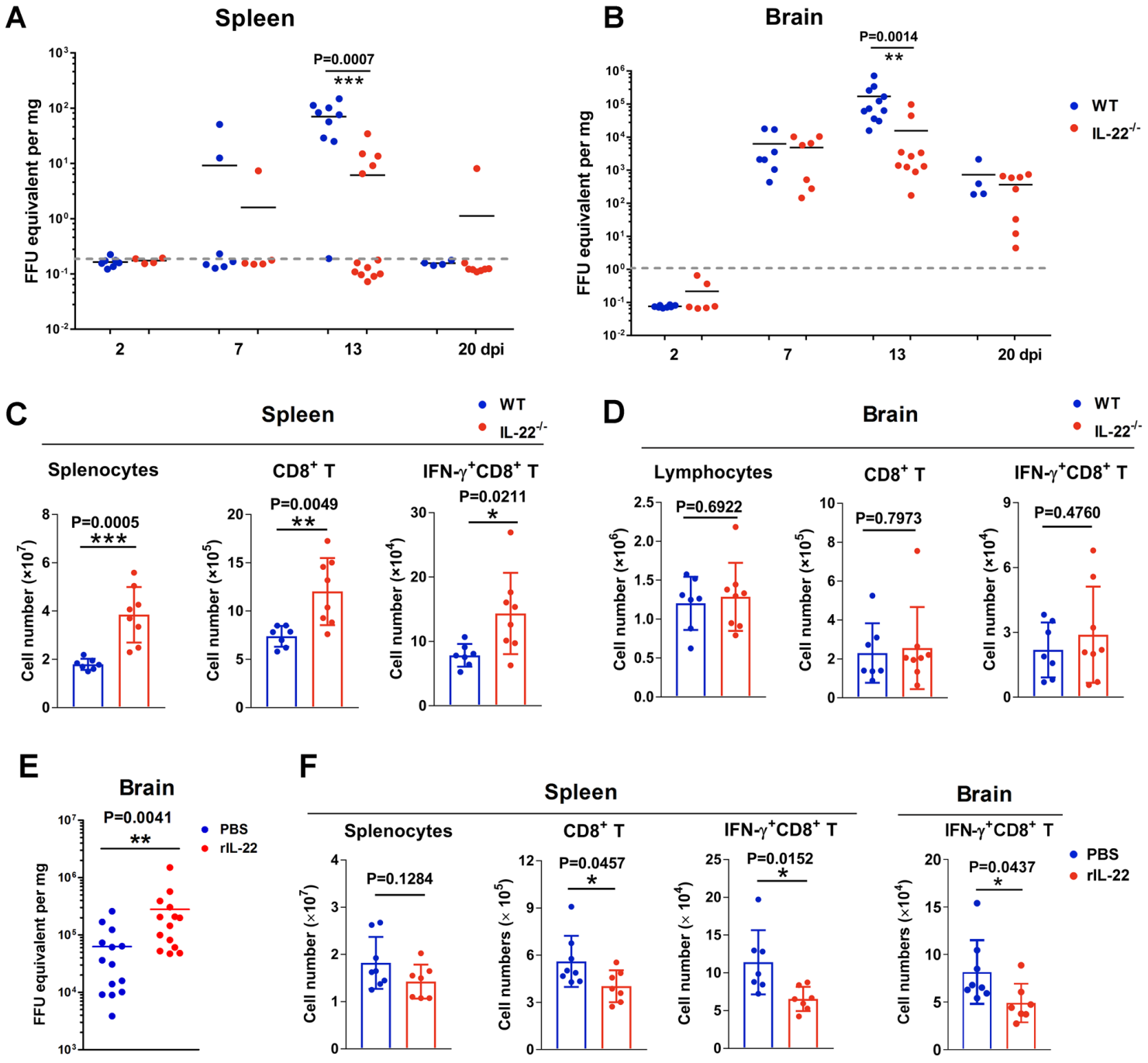


Figure 5

IL-22 dampens anti-ZIKV CD8+ T cell responses. Neonatal WT and IL-22-/- mice were s.c. infected with ZIKV. (A and B) Viral loads of the spleen and brain were measured at 2, 7, 13 and 20 dpi. (C and D) Lymphocytes were harvested from the spleen and brain at 13 dpi and stimulated with ZIKV peptide for 5 hrs in the presence of Brefeldin A. ZIKV-specific CD8+ T cells were quantified by intracellular flow cytometry staining. (E) Neonatal WT mice were s.c. infected with ZIKV, followed by rIL-22 treatment as

indicated in Figure 2E. Viral loads of brains were measured at 13 dpi, and (F) ZIKV-specific CD8+ T cells were quantified in the spleen and brains. All experiments were repeated three times independently. Data are shown as means ± SEM and a two-tailed Student's t-test was used for statistical analysis. * P<0.05, ** P<0.01, *** P<0.001.

Supplementary Files

This is a list of supplementary files associated with this preprint. Click to download.

- TableS105052020.docx
- Supplementarydata.docx